



The Society shall not be responsible for statements or opinions advanced in papers or in discussion at meetings of the Society or of its Divisions or Sections, or printed in its publications. Discussion is printed only if the paper is published in an ASME Journal. Released for general publication upon presentation. Full credit should be given to ASME, the Technical Division, and the author(s). Papers are available from ASME for nine months after the meeting.
Printed in USA.

Copyright © 1985 by ASME

Development of Small Rotating Stall in a Single Stage Axial Compressor

K. MATHIOUDAKIS and F. A. E. BREUGELMANS
von Karman Institute for Fluid Dynamics
Chaussée de Waterloo, 72
B-1640 Rhode Saint Genèse—Belgium

ABSTRACT

In this paper we present the results of a detailed experimental study of the development of small rotating stall, as it appears in a one stage axial compressor. Stationary hot-wire probes are used to measure the variation of amplitude and propagation speed of the disturbances caused by small stall. Measurements near the rotor blade surface with rotating probes provide additional information on the nature of the phenomenon. The development of the cell pattern for different operating conditions is studied. The different character from what is known as "big stall" is demonstrated.

NOMENCLATURE

c	chord
E	power spectral density function
f	frequency
h	distance from hub in percentage of span
n	number of cells, circumferential harmonic number
P	pressure
$(t/c)_{\max}$	(maximum thickness)/(chord) of a blade section
u	velocity component sensed by thermal tuft
U	peripheral velocity
V	absolute velocity
ω	speed of rotation
α	absolute flow angle
φ	blade camber angle
ϕ	flow coefficient V_a/U_T
ψ_{TS}	load coefficient $(P_{st,exit} - P_{t,inlet}) / (1/2 \rho U_T^2)$
γ	percentage of the time the flow moves from the leading to the trailing edge, stagger angle

Subscripts

a	axial
m	mid radius
r	rotating frame
R	rotor
s	stationary frame
T	tip

Superscripts

- time averaged quantity
- ' fluctuating component $q' = q - \bar{q}$

INTRODUCTION

The performance of axial flow compressors at reduced flow rates is characterized by the occurrence of unsteady flow phenomena, namely rotating stall and surge. When surge happens global oscillations of the mass flow occur. When rotating stall happens one or more zones, called rotating stall cells, with reduced or no through flow develop and rotate around the circumference at a fraction of the compressor rotational speed. Even if this phenomenon has been first observed about 40 years ago and is of great importance for the definition of the operating range of a compressor, not very much is known about its physical mechanism.

In the early experimental research [1-6] the appearance of two types of rotating stall was already reported. The first showed small amplitude fluctuations of the angle and the velocity magnitude (small stall) and usually appeared with a big number of cells. The second showed very big changes of flow parameters inside the cells (big stall) and a small number, usually 1 or 2 cells. Similar observations were done in recent investigations [7,8]. While big stall has been investigated in detail recently [9], the small stall has not received much attention.

The existence of a difference in the physical mechanism of the two types of stall implies that theoretical modelling should take into account the particular characteristics of each case. For example, the existing small perturbation analysis models could be suitable for small stall while they cannot provide any information on the occurrence or the characteristics of big stalls. For that case modelling should start from fundamentally different considerations.

In order to understand better the physics of the two cases a detailed investigation of each is necessary. A step towards this direction was already taken by the present authors in [8], where some flow measurements were presented for the two cases and their difference was pointed out. In the present work we give the

results of a detailed investigation for the case of appearance of small stall. Results from stationary and rotating instruments provide information on the occurrence and development of it. Conclusions on the physical mechanism of the phenomenon are drawn.

FACILITY, INSTRUMENTATION AND TECHNIQUES

LOW SPEED AXIAL FLOW COMPRESSOR R 1

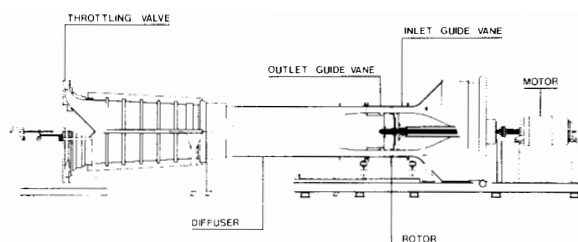


FIG.1 - THE TEST COMPRESSOR

The experimental investigation reported here is carried out in a low speed axial flow compressor consisting of inlet guide vanes (IGV), rotor and stator, shown in figure 1, with a design flow coefficient of $\phi = 0.5$. The outer diameter of the test section is 0.704 m and the hub-tip ratio is 0.78. The distance between IGV trailing edge and rotor leading edge is 0.094 m and between rotor and stator 0.069 m, at mid radius. The geometric data for IGV and rotor blades are given in Table 1. The stator blades are 25 constant thickness, non twisted, thin metal airfoils of 35° camber and 34° stagger, constant chord of 0.080 m and $t/c = 0.025$.

Blade shape : NACA 65 ($C_{2.0}A10$)

h	0	0.25	0.50	0.75	1
φ (°)	47.01	44.76	42.55	40.73	38.86
$\left(\frac{t}{c}\right)_{\max}$	0.06	0.06	0.06	0.06	0.06
γ (°)	21.69	20.65	19.63	18.79	17.73
c (mm)	44.5	47.5	50.5	53.5	56.5

a. Inlet guide vane, 39 blades

φ (°)	22.34	18.34	14.83	11.74	9.23
$\left(\frac{t}{c}\right)_{\max}$	0.06	0.06	0.06	0.06	0.06
γ (°)	24.56	31.54	37.33	42.11	46.03
c (mm)	70.4	75.2	80.0	84.8	89.6

b. Rotor, 25 blades

TABLE 1 - GEOMETRY OF INLET GUIDE VANE AND ROTOR BLADING

Hot wires in different configurations are used for the unsteady measurements. A crossed hot wire probe is used

for measurements in the stationary frame at different axial locations. A V-shaped hot wire sensor is mounted on a rotor blade at 25% of chord from the leading edge at mid-height of the blade. Eventually a thermal tuft consisting of two parallel hot wires is mounted at mid-chord, mid-height of a rotor blade. More information about the sensors is given in [8].

All hot wires are operated in the constant temperature mode, using VKI anemometer bridges. A mercury slip ring transmits signals from sensors on the rotor to the bridges. The bridge voltage outputs are sent to a PDP 11/34 computer by means of a 16-channel data acquisition system. All data processing is then done on the computer. For some of the data a HP-3582A frequency analyzer is used as well.

From the measured voltages the quantities of interest, such as velocities and angles, are derived by using the calibration curves of the corresponding sensor. The traces thus obtained are used for further processing.

The analysis we pursue is based to a large extent on the calculation of power spectral density functions of the signals. These functions are derived from the complex Fourier Transform of the signals calculated by means of a Fast Fourier Transform (FFT) subroutine. Examination of the spectra evaluated in this way gives the frequency of occurrence of periodic variations at those frequencies where peaks are observed. The magnitude of the peaks denotes the relative importance of the corresponding periodic components.

EXPERIMENTAL PROCEDURE

The crossed hot wire probe is placed successively at different axial locations, namely, upstream of the IGV, between the IGV and the rotor, between the rotor and stator and downstream of the stator. With the probe in place the small stall regime is established. The measurements are taken for operating points starting at the appearance of small stall and finishing at its cessation (when big stall starts). Very fine changes in throttling are necessary in order to provide small changes in flow coefficient and describe the corresponding change of the observed pattern. The tests with the probe at different locations as well as with the sensors on the blade are performed separately. When the thermal tuft is used, measurements for the whole operating range of the compressor are taken. For all the experiments the compressor is operating at 1000 RPM. This speed can be kept constant within 0.2%.

For each measuring point 20 samples of 1024 values each are taken for the calculation of the FFTs. The transform of each sample is computed and the average over all the samples gives the final result. The acquisition frequencies are 400 Hz for stationary and 100 Hz for rotating probes and the frequency interval in the FFT calculation is 0.3906 Hz and 0.0488 Hz respectively. The data were low pass filtered at half the acquisition frequencies.

When small stall with many cells is present, a difficulty arises in the accurate determination of the number of cells. The method of inserting two hot wires at different circumferential positions [1] does not give a unique solution. This difficulty was already mentioned in [3] and is due to the non repeatability of the cells themselves. We adopted the following procedure in order to overcome it. The power spectra of signals from a stationary and a rotating probe, taken at the same operating point, are calculated. Peaks corresponding to the passage of the same periodic component from the two sensors can be identified. The sum of the frequencies of these must be a multiple of rotor rotational frequency :

$$f_s + f_r = n \cdot f_R$$

Corresponding peaks in the two spectra are those giving an integer solution for n , which is thus accurately defined. In the results reported here the solution for n deviated from the closest integer by ± 0.03 for corresponding peaks. Non-corresponding peaks gave deviations greater than ± 0.15 from the closest integer.

EXPERIMENTAL RESULTS

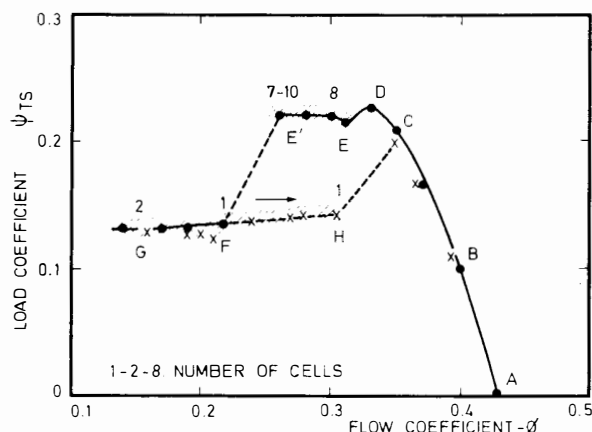


FIG. 2 - THE COMPRESSOR PERFORMANCE MAP

The performance map of the compressor is shown in figure 2. Reducing the flow rate results in an increase of the load coefficient ψ_{TS} up to a maximum value. Immediately after, at $\phi = 0.335$, small amplitude oscillations appear and the performance drops slightly. They persist up to a value of $\phi = 0.26$ and at this point an abrupt drop of ψ_{TS} occurs with big stall appearing. The flow characteristics for different operating regimes as well as the difference between the two kinds of stall were presented in [8]. The results we present here are from measurements in the small stall region, points between D and E'.

Instantaneous velocity and angle traces

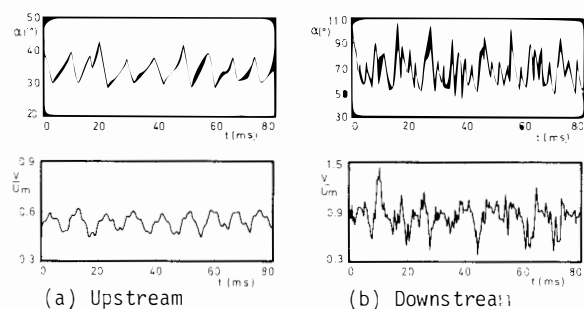


FIG. 3 - INSTANTANEOUS ANGLE AND VELOCITY TRACES UP- AND DOWNSTREAM OF THE ROTOR, AT MID-RADIUS FOR $\phi = 0.310$

In figure 3 the variation of the velocity and angle, up- and downstream of the rotor at mid-radius, is shown for $\phi = 0.310$. The oscillations are of small amplitude around the mean value. The observed non repeatability of the cells is due to the random components of the velocity fluctuations as well as to the content of periodic fluctuations of different frequencies as will be explained in the next section.

Radial traverses were done at the measuring stations up- and downstream of the rotor. Velocity and angle traces for different radial positions given in [8], showed that the stall pattern extends all along the span. (The synchronization of traces at different radial positions, which was done arbitrarily in [8], was verified, confirming that oscillations near the hub are in phase with the ones near the tip). The flow continues to move through the rotor and no radical reorganization of the throughflow was observed, as happens in the case of big stall [8,9].

Power spectra

Power spectra calculated from the axial velocity signals at the mid-height position for different axial locations are given in figure 4. They correspond to

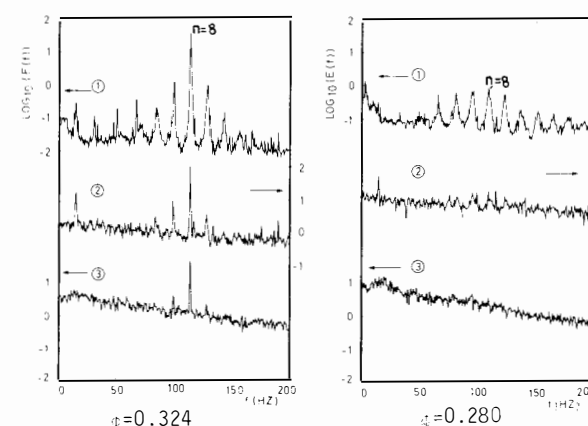


FIG. 4 - AXIAL VELOCITY POWER SPECTRA FOR DIFFERENT AXIAL LOCATIONS. 1: IGV-ROTOR, 2: ROTOR-STATOR, 3: DOWNSTREAM OF STATOR

two flow coefficients, $\phi = 0.324$ at the beginning of the development of the small stall pattern and $\phi = 0.280$ before its cessation.

The spectrum upstream of the rotor for $\phi = 0.324$ shows the existence of several periodic oscillations. Determination of n , as described previously, indicates that the peak with the maximum value corresponds to $n = 8$. Peaks of considerable importance are also observed for $n = 7, 9$ and smaller ones for other numbers. This means that a dominant wave of $n = 8$ exists but the simultaneous existence of other frequencies will modify its shape resulting in the non similarity of the cells among them, as mentioned before. Decrease of ϕ changes the pattern. At $\phi = 0.280$ the values of the peaks are lower, corresponding to smaller amplitudes, and the wave with $n = 8$ is not dominating anymore. It was found that further reduction results in the disappearance of those peaks at the last operating point before the big stall occurrence.

The simultaneous existence of oscillations with wavelengths corresponding to different numbers, explains the ambiguity in cell number determination reported in [3] and elsewhere. An objection that could be raised here is that the appearance of distinct frequencies in the power spectra is a by-product of the frequency averaging process employed. The observed behaviour could result from an intermittency of the cell pattern, if transition between different cell numbers occurs. The simultaneous existence of different circumferential harmonics was confirmed by calculation of the autocorrelation function

of signals, which showed that the pattern remains invariant in time. On the other hand, a modulation of the amplitude of this function within one stall event was observed (an example has been given in [8]), suggesting that the oscillations are composed from harmonics of neighbouring frequencies corresponding to the different n .

Similar observations can be done for the spectra downstream of the rotor. For $\phi = 0.324$ the wave with $n = 8$ is dominant while the only other peaks appearing are for $n = 7, 9$. The amplitudes of other periodic components is probably of the same level as random turbulent flow disturbances and cannot be distinguished from them. The area under the spectra is higher than upstream. This means that the turbulent kinetic energy in the low frequency range is higher than upstream. Separated flow from the rotor blades contributes to this effect. The same comments are valid for the results downstream the stator. Application of the processing on signals from measurements upstream of the IGV showed that the pattern was hardly observed there.

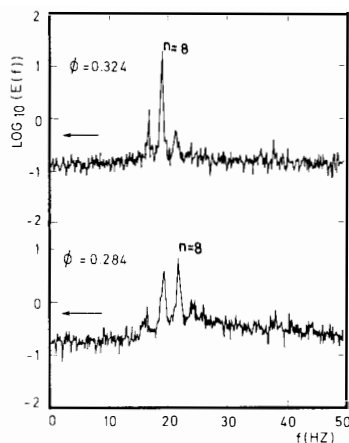


FIG. 5 - POWER SPECTRA OF VELOCITY FROM THE SENSOR ON THE BLADE

In figure 5 the power spectra of velocity measured by the V-shaped sensor on the blade are shown. The only periodicities sensed near the blade surface correspond to $n = 7, 8, 9$. A similar behaviour to the absolute frame is seen: the wave with $n = 8$ initially dominates, while at lower ϕ the $n = 7$ one becomes of the same order of magnitude.

Disturbance amplitude variations

The variation of the amplitude of oscillations in axial velocity upstream the rotor for different n , calculated by power spectra measurements, is presented in figure 6. For a certain flow coefficient the dominant wave is the one with the maximum amplitude. For $\phi > 0.3$ the wave with $n = 8$ is dominant; for $\phi < 0.3$ the $n = 7$ becomes of the same order. The amplitudes for the other numbers have initially much smaller values while they become relatively more important as ϕ is decreasing. As the flow coefficient is reduced amplitudes initially increase reaching a maximum (at $\phi = 0.320$ for $n = 8$), dropping then again to smaller values.

The evolution of the amplitude for the 8 cell oscillation for different axial locations is shown in figure 7. The same trend is observed for all locations.

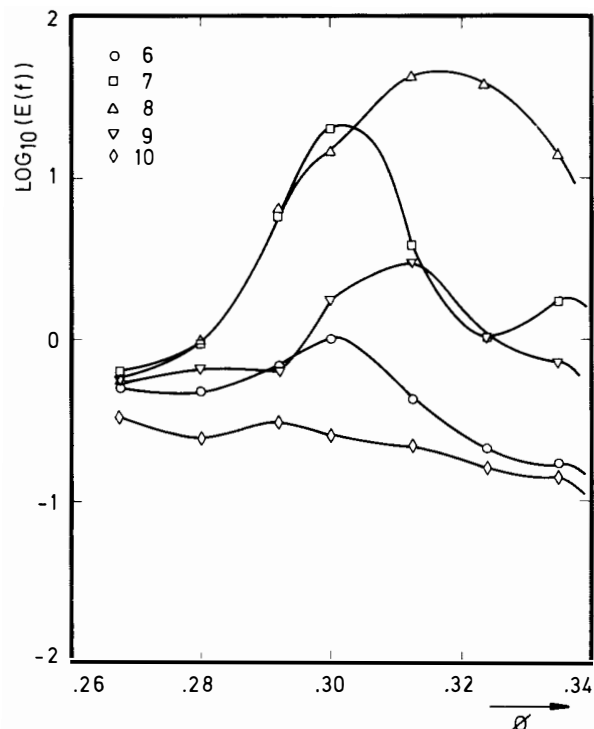


FIG. 6 - RELATIVE AMPLITUDE OF AXIAL VELOCITY OSCILLATIONS UPSTREAM OF THE ROTOR FOR DIFFERENT n

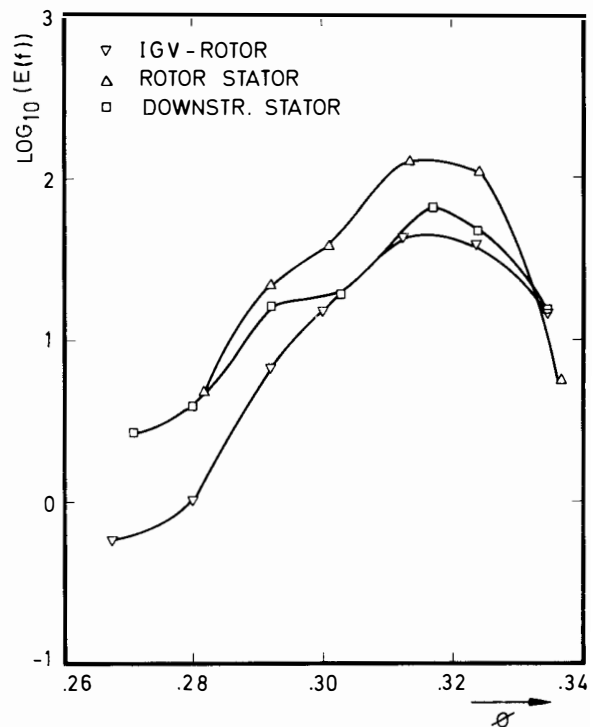


FIG. 7 - AMPLITUDE OF AXIAL VELOCITY OSCILLATIONS WITH $n = 8$ FOR DIFFERENT AXIAL LOCATIONS

The values downstream of the rotor are higher than the ones upstream. The rotor amplifies the disturbances. They are attenuated showing lower amplitudes at the location downstream of the stator. Examination of amplitudes for different n showed a trend similar to the one of figure 6 for the other two axial locations as well.

Propagation speed

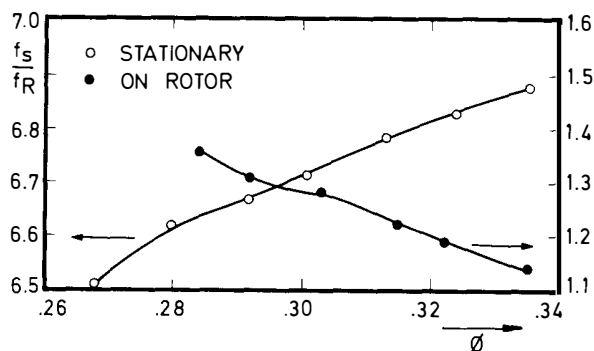


FIG. 8 - FREQUENCIES FOR $n = 8$ IN THE ABSOLUTE AND RELATIVE FRAME

During the change of ϕ a shift of the frequency of the peaks is observed indicating a change in the propagation speed of the cells. In figure 8 the variation of the frequencies corresponding to $n = 8$ as observed from the stationary and the rotational probes are plotted versus flow coefficient. They are complementary with respect to the rotor frequency of rotation. Cell frequencies were also found to be proportional to rotor frequencies for the same throttle setting at different rotor speeds. In figure 9 the propagation speeds in

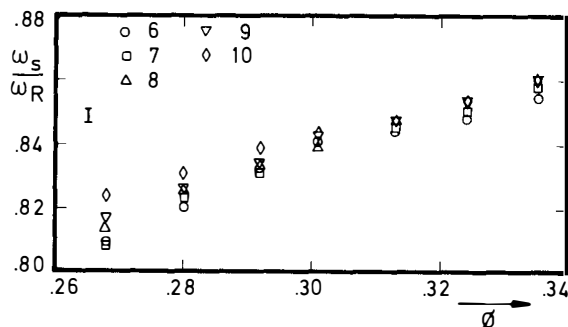


FIG. 9 - PROPAGATION SPEED OF OSCILLATIONS FOR DIFFERENT n

the absolute frame for different n are plotted. The accuracy in the definition of the speed is limited by the frequency interval in the FFT. For a certain ϕ with $0.30 < \phi < 0.34$ the propagation speed is the same for all n within the accuracy of the measurements. For $\phi < 0.30$ small differences are observed. For a certain n the speed decreases monotonically with ϕ and this is the same for all n . Radial traverses in front of the rotor showed that propagation speed is the same along the blade height.

On blade flow

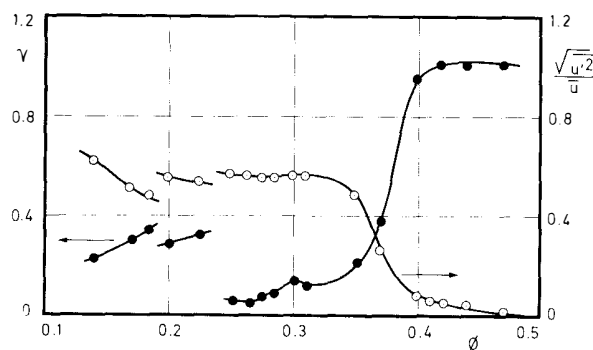


FIG. 10 - THERMAL TUFT RESULTS

As discussed in detail in [10] the thermal tuft sensor can detect the percentage of the time γ that the flow moves in the nominal direction, namely from the leading to the trailing edge of the blades. The variation of this ratio for values of ϕ covering the whole operating range of the compressor is shown in figure 10. In the same figure the velocity fluctuations (component perpendicular to wires) are shown. For clean flow conditions $\gamma = 1$, meaning that near the blade surface a two dimensional through flow pattern is expected. At $\phi = 0.400$ the value starts dropping indicating a thickening of the rotor blade boundary layer with its three dimensional features intensified. At $\phi = 0.335$ a value of 0.15 is reached when the small stall regime starts. This value is kept almost constant through the whole small stall region. This means that the flow has almost permanently deviated from the nominal direction to some three dimensional, maybe separated pattern. While in clean flow velocity fluctuations keep very small values, in the small stall region a very high level is observed which is not changing much over that region. This is another indication of separated flow in this operating region.

Further throttling, when big stall occurs, results in an increase of γ to a value corresponding to the circumferential extent of the big cells. The behaviour is completely different [8]. Part of the time the flow moves in the nominal direction (clean flow) and part of the time it is deviating from it (stall cells). During the small stall the flow near the blade surface shows a rather permanent deviation from clean flow operating conditions. The existence of a periodic variation was nevertheless found (power spectra measurement gave peaks at the same frequencies as the V-shaped sensor). This is a result of the interaction with the main oscillating flow.

DISCUSSION

The phenomenon of small rotating stall is not a particular feature of the compressor used in the present study. It has been observed in a number of different compressor investigations which we report below. Small amplitude, rotating, self induced oscillations were observed in stationary annular cascades [2]. Their development was attributed to boundary layer growth and separation and their difference from big rotating stall was pointed out. Different patterns of rotating stall, identified to be of the small stall type, in single stage axial compressors have been reported in [1,3,5,6,7]. Hub-tip ratios in these compressors were varying from

0.5 [5] to 0.85 [7]. Many cells rotating at relatively high speeds was a common feature of those observations. Eventually multiple stall cell configurations of a mild character have been reported to occur in multistage aeronautical compressors [11]. The lack of detailed data for this last case precludes a definite conclusion on whether the cells are of the small type or not. Although the phenomenon has been observed in all those different cases, no quantitative description has been given in any of them. We discuss now some of the observations in our compressor.

The performance of the compressor is dropping gradually when small stall appears. It was found in [9,12] that gradual drop in the performance can be linked to the appearance of big cells covering a part only of the blade height. For this reason the term "small stall" was preferred to the usual one of "progressive stall", as more precise. The fact that the fluid keeps moving through the compressor without radical reorganization, implies that the occurrence of small stall at an intermediate stage of a multistage machine will be seen as a flow distortion for the rest of the stages. Depending on their operating point they can amplify or attenuate this distortion [13]. In the second case a stall pattern covering only a few stages will appear. Such a case was mentioned in [11], where a pattern of 7 cells covering only the front stages of a multistage aeronautical compressor has been reported.



FIG. 11 - HOT WIRE TRACES DOWNSTREAM OF THE ROTOR

The occurrence of small stall seems to be linked to the occurrence of separation on the rotor blades. This is suggested from the thermal tuft results of figure 10. The occurrence of separation on the blade is confirmed from observation of hot wire traces behind the rotor blade trailing edge. Such traces at mid-height position and different points on the performance map are shown in figure 11. It is seen that after point D, where small stall starts, the flow is separated. Radial surveys, showed also that before stall starts separation has already started in the upper part of the blade. Reducing the flow rate resulted in an expansion of the separated region towards the hub. At $\phi = 0.330$ the flow separated along the whole span. This stayed the same until the occurrence of big stall. It is concluded that the onset

of small stall is triggered by the appearance of separation on the rotor blades. This is not valid for the occurrence of big stall, which started well after the flow separated along the whole blade span. This implies that explanations and models based on the blade profile boundary layer separation should be restricted to the small type, the big one being due to other reasons, probably related to the overall stability of the flow (see also [17]) and three dimensional phenomena.

In most existing theories the onset of the stall, whatever the type, is supposed to coincide with the amplification of small perturbations (only in [6] the two types are treated in different ways). While this is valid for small stall it is not true for the big. As shown by our data small disturbances are much less amplified just before big stall occurrence, in comparison to the amplification at some previous value of ϕ where a maximum occurred. Such a criterion should not then be expected to give a correct prediction for big stall and another one should be used.

Concerning the description of the stall cell pattern we showed that it is not entirely correct to speak about a pattern by referring to only one number of cells. This can be done if a predominant wave is observed and even then, important periodic components corresponding to other numbers can exist. It would be preferable to talk about the relative importance of oscillations corresponding to the different cell numbers. It was demonstrated that identification of these numbers for a certain pattern can be done by using power spectral analysis and not at all by inspection of traces. Another feature related to this behaviour is that change in number of cells does not happen abruptly as in big stall. In the latter case a sudden change of the number of cells occurs at a certain value of the flow coefficient [8]. Here a progressive evolution of amplitudes is observed instead. A change in cell number occurs if a wave with a different length becomes predominant. In [14] a theoretical model for propagation of small perturbations in multistage compressors predicted this type of behaviour. The possibility of amplification of disturbances at different frequencies was demonstrated. The harmonic with the frequency at which the maximum amplification occurred was defined as the number of cells. The importance of other frequencies was disregarded as no experimental evidence on such behaviour existed before.

Small perturbation theories could be used to study small stall, as their assumption for small amplitude are fulfilled in this case. A conclusion of these types of theories [15,16] is that stall will occur at the point of the performance map where $d\psi_{TS}/d\phi = 0$. This is not true for big stall as has been discussed in detail in [17]. In our case the performance curve shows in fact that $d\psi_{TS}/d\phi = 0$ over the whole small stall region verifying the prediction of small perturbation theories. When such a theory is employed, care must be taken in the modelling of the blade rows. Two dimensional cascade models do not seem very promising. In our case, for instance, the fact that the rotor blades are twisted (tip section by 22° with respect to the hub) would imply that different stall characteristics will be exhibited along the blade height if such a model is used. Propagation speeds calculated with the formula derived in [2], applied on the rotor alone, show a variation of 20% along the height while we observed the same propagation speed. A global model of the flow taking into account spanwise variations should be used for a correct prediction.

Finally similar type of stall has also been observed in centrifugal compressors. In [18] the appearance of two distinct types of impeller stall was demonstrated. The type named "progressive" there seems to exhibit the same properties as our small stall and is attributed

to boundary layer growth and separation as well.

CONCLUSIONS

An experimental study of the detailed flow characteristics of small rotating stall in axial compressors has been presented. The difference in terms of flow behaviour and inception criteria from "big rotating stall" was pointed out. A way of determination of the number of cells in multicell configurations is suggested.

The main conclusions on the development of small rotating stall can be summarized as follows : Small rotating stall is attributed to blade boundary layer separation and interaction with the blade passage inviscid flow. The rotating pattern can be characterized by the simultaneous existence of disturbances of different wavelengths. The classical way of talking about a number of cells should thus be substituted by defining the relative amplitudes at different wave numbers. These amplitudes are found to change with the operating point. The propagation speed is found to be decreasing with reducing the flow coefficient.

Review of previous experimental studies showed that this phenomenon is encountered in a variety of compressor configurations. Small perturbation theories could be suitable for its study.

REFERENCES

1. Huppert, M.C.: Preliminary investigation of flow fluctuations during surge and blade row stall in axial flow compressors. NACA RM E52E28, August 1952.
2. Rannie, W.D. & Marble, F.E.: Unsteady flows in axial turbomachines. ONERA Comptes Rendus des Journées Internationales des Sciences Aéronautiques, Paris 1957.
3. Montgomery, S.R. & Braun, I.J.: Investigation of rotating stall in a single stage axial compressor. NACA TN 3823, January 1957.
4. Stenning, A.H.; Seidel, B.S.; Senoo, Y.: Effect of cascade parameters on rotating stall. NASA Memo 3-16-59W, April 1959.
5. Valensi, J.: Experimental investigation of the rotating stall in a single-stage axial compressor. J. Aero. Sci., Vol. 25, No. 1, January 1958, pp 1-10.
6. Yershov, V.N.: Unsteady conditions of turbodynamics rotating stall. Translated by the Foreign Technology Division of the U.S.A. Ref: FTD-MT-24-04-71.
7. Tanaka, S. & Murata, S.: On the partial flow rate performance of axial flow compressors and rotating stall. Bull. JSME, Vol. 18, No. 117, March 1975, pp 256-271.
8. Breugelmans, F.A.E.; Mathioudakis, K.; Casalini, F.: Flow in rotating stall cells of a low speed axial flow compressor. 6th ISABE, Paris, June 1983. Also VKI Preprint 1982-27.
9. Day, I.J. & Cumpsty, N.A.: The measurement and interpretation of flow within rotating stall cells in axial compressors. J. Mech. Eng. Sciences, Vol. 20, No. 2, 1978, pp 101-114.
10. Ligrani, P.M.; Gyles, B.R.; Mathioudakis, K.; Breugelmans, F.A.E.: A sensor for flow measurements near the surface of a compressor blade. J. of Physics E : Scientific Instruments, Vol. 16, No. 5, May 1983, pp 431-437. VKI Preprint 1983-19.
11. Freeman, C. & Dawson, R.E.: Core compressor development for large civil jet engines. 1983 Tokyo Int. Gas Turbine Congress, Oct. 1983, Paper 83-Tokyo-IGTC-46.
12. Dunham, J.: Observation of stall cells in a single stage compressor. ARC CP 589, March 1961.
13. Stenning, A.H.: Inlet distortion effects in axial compressors-rotating stall and surge. ASME Trans., Series I - J. Fluids Engrg., Vol. 107, No. 1, March 1980, pp 7-20.
14. Ferrand, P. & Chauvin, J.: Theoretical study of flow instabilities and distortions in axial compressors. ASME Trans., Series A - J. Engrg. for Power, Vol. 104, No. 3, July 1982, pp 715-721.
15. Dunham, J.: Non-axisymmetric flows in axial compressors. Mech. Eng. Science, Monograph N° 3, October 1965.
16. Moore, F.K.: A theory of rotating stall of multi-stage axial compressors : Part 1 : Small disturbances. ASME P 83-GT-44, 1983.
17. Koff, S.G. & Greitzer, E.M.: Stalled flow performance for axial compressors. I : Axisymmetric characteristic. ASME P 84-GT-93, June 1984.
18. Frigne, P. & Van den Braembussche, R.: Distinction of different kinds of impeller and diffuser rotating stall in a centrifugal compressor with vaneless diffuser. ASME Trans., Series A - J. Engrg. for Gas Turbines and Power, Vol. 106, No. 2, April 1984, pp 468-272. Also VKI Preprint 1982-39.